RSC Advances

ROYAL SOCIETY OF CHEMISTRY

www.rsc.org/advances

Characterization of various experimental parameters leads to optimized conditions for depositing linear strings of gold nanoparticle seeds on DNA origami.

Nanoscale

RSCPublishing

ARTICLE

Optimizing Gold Nanoparticle Seeding Density on DNA Origami

Cite this: DOI: 10.1039/x0xx00000x

E. P. Gates,[a] J. K. Jensen,[a] J. N. Harb[b] and A. T. Woolley[a]

Received 00th September 2014,
Accepted 00th September 2014

DOI: 10.1039/x0xx00000x

www.rsc.org/nanoscale

DNA origami is a valuable technique in arranging nanoparticles into various geometries with a ~100 nm footprint, high resolution, and experimental simplicity. Aligned nanoparticles, in addition to being used for photonics, can also be utilized to create thin metal wires with intricate and asymmetric junctions. Many factors affect the yield and density of nanoparticles attached to DNA origami structures, including the length and number of attachment sequences, the reaction ratio of nanoparticles to DNA origami, the hybridization temperature, and age of the solutions. This work investigates the alignment of closely packed 5 nm gold nanoparticles along thin DNA origami structures. Several reaction conditions, including hybridization time, magnesium ion concentration, ratio of nanoparticles to DNA origami, and age of the nanoparticle solution, were explored to optimize nanoparticle attachment density and spacing. Optimum ranges of conditions were identified, yielding new insights into high-density nanoparticle attachment to thin DNA origami structures, with potential for application in nanowire and nanoelectronics construction.

Introduction

Scaffolded DNA origami[1] is a versatile, one-pot system for creating designed ~100 nm scale nanostructured objects. It has been used to create complex two-[2-4] and three-dimensional[5-8] structures as well as to organize nanomaterials.[9-22] Nanoparticle attachment to DNA origami offers a desirable bottom-up self-assembly process. The DNA origami allows for specific positioning of nanoparticles, enabling control over both alignment and spacing. Nanoparticles that have been localized on DNA origami include gold,[23-32] silver,[33] and quantum dots.[34, 35] We previously demonstrated the use of positioned gold nanoparticles (Au NPs) as seeds for electroless metal deposition to create conductive nanowires.[30] This approach enables the application of DNA origami templates to form complex nanowire shapes and junctions that would be difficult to assemble with other techniques. In addition, Au NPs precisely positioned along DNA origami ("Au NPs" in conjunction with DNA herein indicates that oligonucleotides are attached to the nanoparticles) could be used to assemble nanostructures for plasmonic nanoantennas,[22] nanolenses,[24] rulers,[31] or circuitry.[32]

Several groups have demonstrated Au NP attachment to DNA origami structures, either through solution[23, 24, 28, 29, 31, 32] or surface seeding,[27] or both.[25, 26, 30] In these reports, various techniques and reaction conditions were reported, including different oligonucleotide attachment lengths (8–30 bases), sizes of Au NPs (5–15 nm), hybridization times (0.3–24 hrs) and temperatures (4–40 °C), and designed distances between the attached Au NPs (10–100 nm). Some researchers used thiolated staple strands to bind to the Au NPs,[23, 26] while many[24, 25, 27-32] used base-pairing of thiolated, oligonucleotide-coated Au NPs to the DNA origami structures. Typically, structures were designed with specific and distinct attachment locations for each Au NP. In some instances, several different sequences[24] or alternating sequences[29, 31, 32] were used. In our approach (Figure 1A),[30] each staple strand in the desired attachment area contains the same protruding oligonucleotide sequence for Au NP-DNA conjugates (all having the complementary sequence) to hybridize with. This strategy allows for increased density of attachment sequences (~6 nm apart) and larger numbers of Au NPs attached to the DNA origami structure, while keeping the number of different thiolated oligonucleotides as low as possible to reduce the cost as well as the complexity in the design. This does, however, raise the challenge that each Au NP does not have a single specific set of staple strands to which it is being tethered. Thus, Au NPs can be bound through hybridization with 2 or more attachment sequences on the DNA origami structures (Figure 1B–E). The Au NPs can also attach in such a way that some hybridization sequences on the DNA origami structures are left unpaired (Fig. 1E) or Au NPs localize with gaps too small to allow an adjacent Au NP to attach with sufficient room or stability (Fig. 1D).

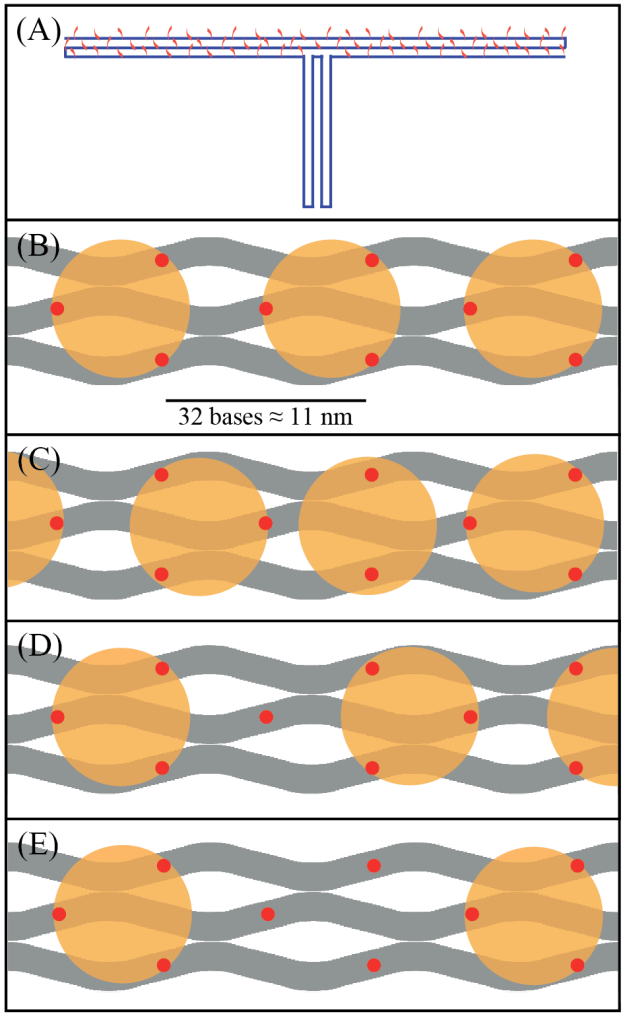

Figure 1. Au NP attachment locations on "T" DNA origami structures. (A) Schematic of "T" DNA origami structure showing red protruding sequences for Au NP attachment along the top section of the DNA structure. (B) Potential Au NP positioning along the DNA origami template with three attachment points per Au NP. (C–E) Other possible Au NP positions along the DNA origami template.

In previous work[30] we showed that 7.6 nm diameter Au NPs could be selectively attached to desired portions of DNA origami templates and used to create conductive nanowires. To achieve the thinnest wires, it is desirable to attach Au NPs as closely as possible along the DNA origami templates. These prior results showed that Au NPs attached to the "T" structures with a median center-to-center distance of ~11.7 nm, yielding a median gap distance of ~4.1 nm. Taking into consideration the observed mean diameter of the Au NPs (~7.6 nm) and the solution length of the thiolated oligonucleotides, the Au NPs were expected to have an effective size of ~11.6 nm, which was nearly identical to the measured median center-to-center distance, as well as the spacing of the attachment sequences on the DNA origami structures. With this effective Au NP size and three attachment positions per Au NP, up to 22 Au NPs can theoretically be attached in a single line along the top of the "T" structure. These results indicate that the Au NPs often packed closely along the DNA origami structures; however, some gaps were also observed. For each of the structures evaluated, there appeared to be at least one larger gap whose distance ranged from 12–37 nm. Since the Au NPs can attach closely in some places, it is desirable to optimize the Au NP attachment process to reduce the size of these gaps or eliminate them entirely.

Factors that can influence the yield of Au NP attachment to DNA origami include: the number of staple strands per Au NP binding site, the length of the attachment sequence, the ratio of Au NPs to DNA origami, the hybridization temperature, and the age of the Au NP solution. Ding et al.[24] reported a decrease in Au NP attachment with only two DNA attachment strands per Au NP binding site when compared with three attachment strands for specifically spaced Au NPs of varying size. Hung et al.[25] studied the effects of the linker length, concentration ratio of Au NPs to DNA origami, and the hybridization temperature. They found that 8-base polyT linkers in place of 30-base polyT linkers, increasing the Au NP concentration from 10 nM to 200 nM relative to the DNA origami structures, and increasing the temperature from 23 °C to 37 °C resulted in higher attachment yields. The best Au NP attachment yields came from solution seeding at 37 °C with T_8 coated Au NPs. The Au NPs in the work of Hung et al.[25] were directed to the corners of triangular DNA origami structures; while the Au NPs were very ordered, they were also far apart instead of densely attached as in our approach. Kuzyk et al.[29] reported optimized conditions for Au NP attachment giving yields of 96–98% per particle; they found it necessary to use the thiolated DNA-coated Au NPs immediately after filtering to prevent unbound thiolated oligonucleotides from binding to the DNA origami structures and decreasing the Au NP attachment yield. In the work of Kuzyk et al.[29] 9 Au NPs were positioned along 1.5 helical turns of a 57 nm pitch helix wrapped around 34 nm diameter DNA origami nanotubes (~180 nm total path length). While aspects of Au NP attachment in each of the above studies have similarities to our technique, none of the prior publications provides a systematic study of linear, dense packing of Au NPs onto DNA nanostructures, investigating the effects of all the experimental factors we have studied.

Here, we systematically explore the effect (on closely spaced Au NP attachment) of hybridization time, magnesium ion concentration, concentration ratio of Au NPs to DNA origami, and the age of the Au NP solution. In order to gauge which reaction conditions provided better Au NP patterned DNA origami structures for future metallization into conductive wires, three different parameters were measured: (1) the total number of Au NPs attached to DNA origami structures, (2) the number of Au NPs in a single-file line along the structures, and (3) the largest gap between neighboring Au NPs in each DNA origami structure. These three parameters are important because if the structures have more Au NPs associated with them than are needed to form a single-file line or if there are large gaps between Au NPs that would need to be filled with metal during plating to make the wire continuous, then wider nanowires would result compared to ones formed through ideal Au NP attachment. These studies offer insights into the Au NP attachment process, detailing optimal conditions for high-density linear alignment of Au NPs on DNA origami structures, which should lead to thinner and more continuous metal nanostructures after plating.

Experimental

Process Overview

We used the branched, "T" DNA origami structure reported previously[30] with modified staple strands for Au NP attachment along the entire top section of the "T". Figure 2 outlines the Au NP attachment process; additional experimental details can be

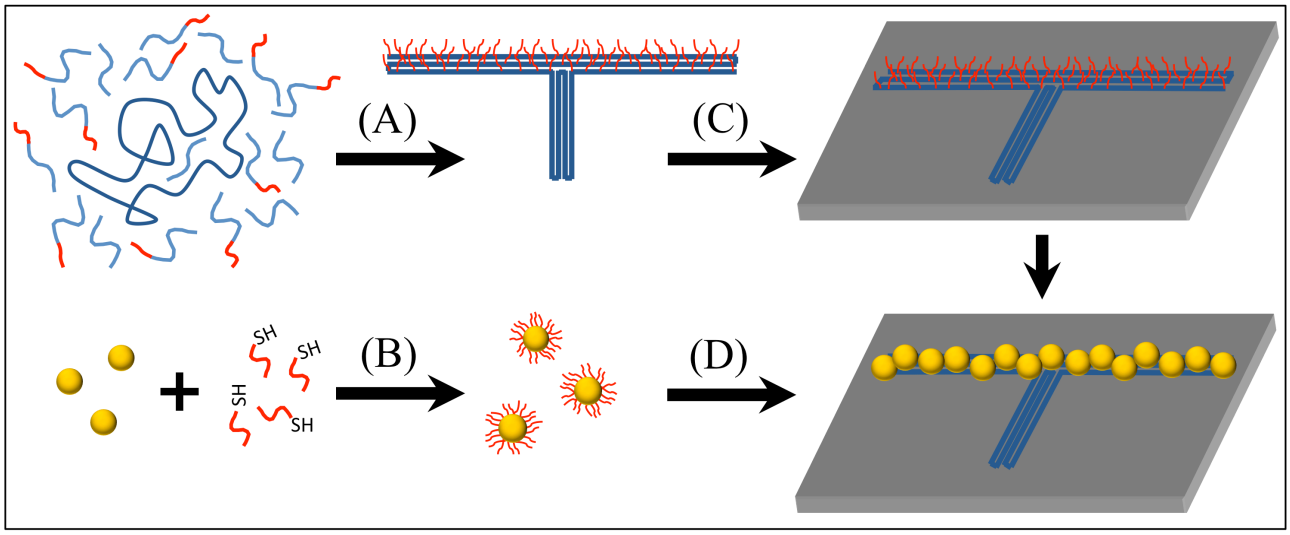

Figure 2. Overview of Au NP attachment process. (A) "T" DNA origami templates are assembled with Au NP attachment sequences (red) along the top section. (B) Au NPs are reacted with thiolated oligonucleotides. (C) DNA origami templates are deposited on silicon oxide surfaces and (D) DNA-coated Au NPs base pair with attachment sequences on the DNA origami structures to form the DNA-templated Au NP nanostrings.

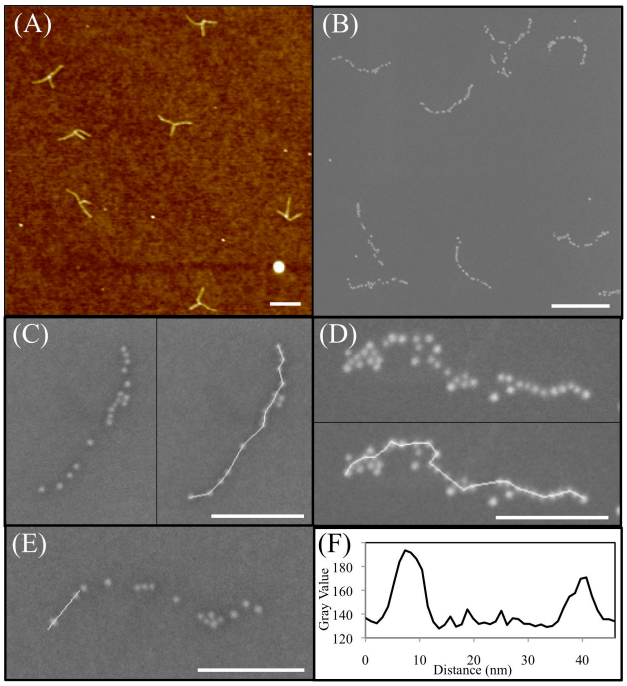

Figure 3. Analyzing Au NP attachment to DNA origami. (A) AFM image of "T" DNA origami structures. (B) SEM image of Au NP seeded DNA structures. (C–D) Examples of SEM data for determining the number of nanoparticles in a line for seeded structures (with and without the line). (E) Example of SEM data for largest gap determination using Image J. (F) Cross-section plot of the line drawn in (E). Scale bars in (A–B) are 200 nm, and scale bars in (C–E) are 100 nm.

found in the Electronic Supporting Information (ESI). The "T" DNA origami structures were folded (Figure 2A), and then filtered to remove excess staple strands. Concentrated, BSPP-coated Au NPs (5 nm) were reacted with an excess of thiolated oligonucleotides (Figure 2B) and then filtered to remove excess unbound DNA. Next, the filtered DNA origami solution was diluted, adjusted to have a higher Mg^{2+} concentration (40–130 mM), and then placed on freshly plasma cleaned silicon oxide surfaces (Figure 2C). The DNA origami structures were allowed to absorb on the surface for 5 min and then the Au NP-DNA solution was added to allow hybridization with the "T" DNA origami structures (Figure 2D). This Au NP attachment method is different from the process reported in our previous work,[30] allowing good surface adherence of DNA origami structures to silicon oxide surfaces, but in fewer steps and significantly less time, due to the higher Mg^{2+} concentration in the DNA origami solution.

AFM/SEM Imaging

AFM imaging of samples was performed in air using tapping mode on a Digital Instruments Nanoscope IIIa MultiMode AFM (Veeco) with silicon force modulation AFM tips (AppNano FORTA probes, 1.6 N/m, 61 kHz). Samples were also imaged with an FEI Helios Nanolab 600 SEM using ultra high resolution, immersion mode.

Results and Discussion

An AFM image is shown in Figure 3A of "T" DNA origami structures before Au NP attachment. An SEM image of Au NP seeded DNA origami structures is shown in Figure 3B. Because the DNA origami structures were designed for the Au NPs to attach only along the top section of the "T" structure, they appear as linear Au NP strings in the SEM images.

SEM images were used to analyze the Au NPs in the attachment studies. The Au NPs in the images were counted and recorded as the total number of Au NPs associated with a nanostring. Additionally, the number of Au NPs on a line along the length of the DNA origami structure was measured. This latter measurement was more complex because the nanostrings are somewhat flexible and are not always linear on the surface. To account for nanostring curvature, the Au NPs did not need to be in a straight line, but were counted following a single-file path through the nanostring (i.e., Figure 3C–D). If Au NPs appeared to be attached two or more wide in places, any extras

were left out of the single-file count. Representative SEM images for the Au NP in-a-line counts are shown in Figure 3C–D. For each of the samples prepared under different conditions, 30 nanostructures were evaluated. To measure the largest center-to-center distance between neighboring Au NPs in each of the DNA origami structures the program *Image J* was utilized. The scale in pixels/nm for each image was set using the scale bar within the SEM image and then a cross section of the two Au NPs was taken to determine the center-to-center distance (Figure 3E–F). The data were adjusted to Au NP spacing distances by subtracting the average Au NP diameter (7.6 nm).[30]

Au NP Attachment Studies

Initial tests of the Au NP attachment process were performed to give starting volumes and concentrations for the DNA origami (5 μL, 1 nM) and Au NPs (20 μL, 10 nM). These volumes and concentrations ensured good coverage of the surface and a ratio of 40:1 Au NPs to DNA origami structures. If the Au NPs attach to the DNA origami structures at three positions per Au NP, then ~22 Au NPs are expected to attach to the top portion of the "T" structure, such that a ~1.8 fold excess of Au NPs was utilized in most of the test studies.

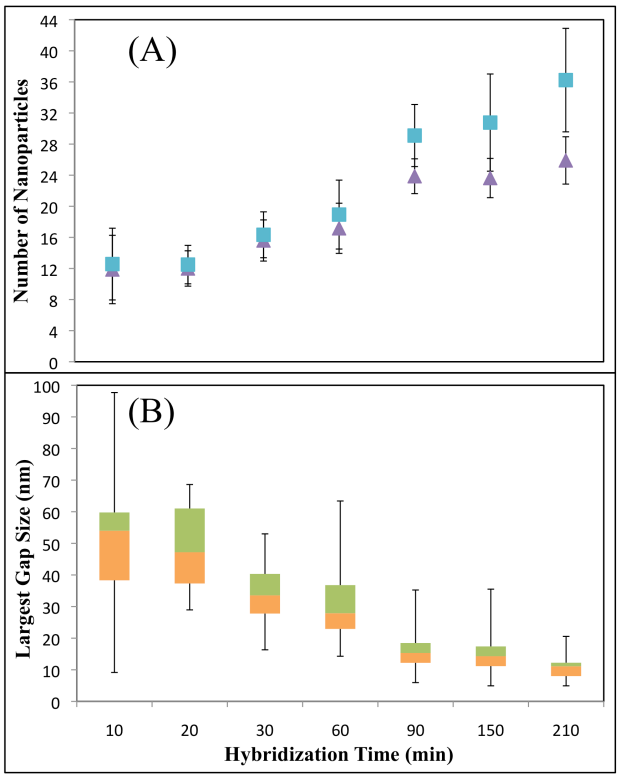

Figure 4. Au NP attachment results for different hybridization times. (A) Graph of the average number of Au NPs attached along a line (purple triangles) and the average total number of Au NPs per nanostring (blue squares). (B) Box and whisker plot of the largest gap between neighboring Au NPs in each string. Thirty nanostrings were evaluated for each hybridization time.

To evaluate the effect of hybridization time on Au NP attachment, the Au NP solution was allowed to react with the DNA origami coated surfaces for times ranging from 10 to 210 min. Figure 4, and Table S1 in the ESI, show the results. For nanoparticle density, hybridization times less than 30 min are insufficient for the desired number of Au NPs to attach, but hybridization times of 90 min or longer show an increasing difference between total NPs and NPs in a line. This separation indicates that the nanostructures are becoming wider than single-file with longer hybridization times.

The largest gap data for the various hybridization times is shown in Figure 4B as a box and whisker plot. As expected, with increasing hybridization time the average largest gap between neighboring Au NPs becomes smaller and has a smaller spread. As shown in Figure 1B, if each Au NP is attaching to the DNA origami through three attachment sequences, the center-to-center spacing of the Au NPs is expected to be ~11 nm with an average distance of 4 nm between edges of neighboring Au NPs. The smallest observed maximum gap size of 5 nm (at 150 and 210 min) indicates that it is possible to place Au NPs along a nanostructure close to this ~4 nm minimum distance between Au NPs. A hybridization time of 90 min appears to be the optimum condition for high linear Au NP density and reduction of gap size.

The 10 and 20 min hybridization samples were deposited on silicon pieces with a 200 nm thermal oxide layer. In these samples (and sometimes faintly on the native oxide surfaces) the DNA can be seen as a darker color than the background, due to surface charging in the SEM (Figure 5). In general, the surfaces with the 200 nm thermal oxide were not used for the Au NP attachment tests because focusing the SEM was more difficult, but for those two short hybridization samples it was helpful for counting Au NPs to be able to see where the DNA structures were located. DNA has also been observed in SEM images by others.[24] Other than being able to visualize the DNA in the SEM images, no other differences were observed in using native vs. thermally grown silicon oxide surfaces to deposit the DNA origami and Au NPs.

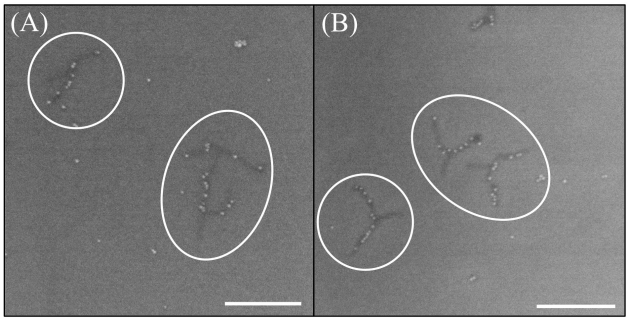

Figure 5. SEM images of Au NP-DNA origami structures on silicon surfaces with a 200 nm oxide layer. (A) Sample hybridized for 10 min. (B) Sample hybridized for 20 min. DNA structures are marked by white circles. Scale bars are 200 nm.

In the next study, the Mg^{2+} concentrations in the DNA origami solutions and the hybridization times were varied. Magnesium ions are important in the formation of DNA origami structures, because they screen the negative charges on the backbone in DNA, allowing the strands to approach closely enough to hybridize. In this work, Mg^{2+} ions also play a role in helping the DNA origami structures adhere to the surface. For the previous hybridization time study, the DNA origami solution was adjusted, after filtering, to contain the desired DNA concentration and 100 mM Mg^{2+}. In the case of the DNA-coated Au NPs, however, extra Mg^{2+} from the DNA origami solution could cause the Au NPs to aggregate when deposited on the surface, leaving fewer Au NPs available for attachment

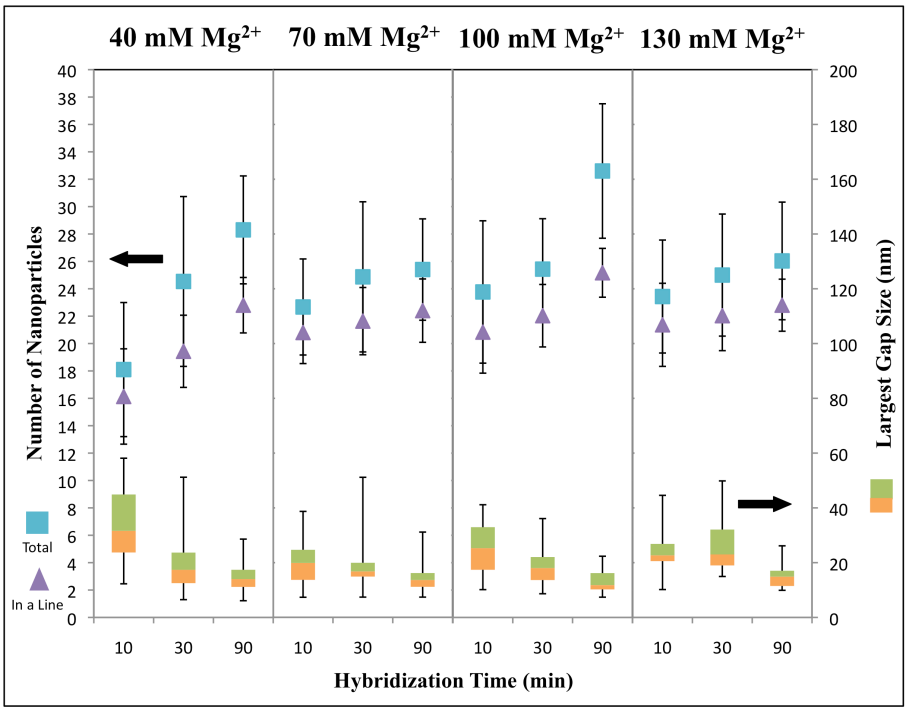

Figure 6. Au NP attachment results with different hybridization times and Mg^{2+} concentrations. Purple triangles represent the average number of Au NPs along a line. Blue squares represent the average total number of Au NPs per nanostring. Orange and green rectangles are a box and whisker plot of the largest gap between neighboring Au NPs in each nanostring. Thirty nanostrings were counted for each hybridization time and Mg^{2+} concentration.

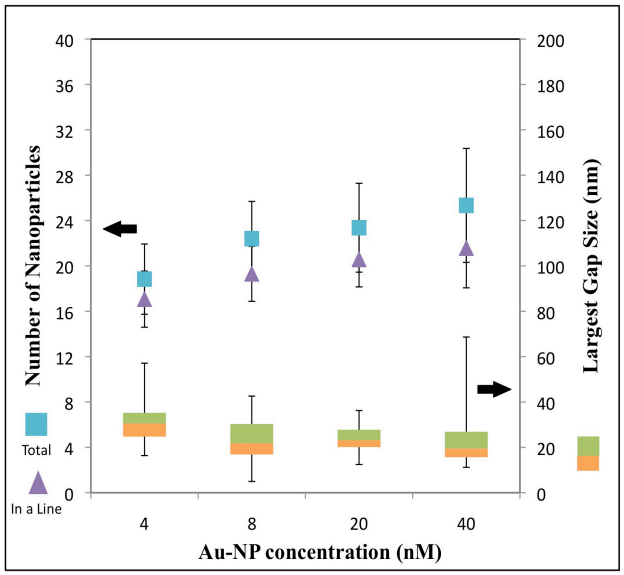

Figure 7. Au NP attachment results with varying Au NP concentrations. Purple triangles represent the average number of Au NPs along a line. Blue squares represent the average total number of Au NPs per nanostring. Orange and green rectangles are a box and whisker plot of the largest gap between neighboring nanoparticles in each string. Thirty nanostrings were counted for each Au NP concentration.

to DNA origami structures or potentially attaching to the DNA origami as clusters or aggregates.

The results for varying Mg^{2+} concentrations and hybridization times are shown in Figure 6, and Table S2 in the ESI. As before, with longer hybridization times more Au NPs attached to the DNA structures. The Mg^{2+} ion concentration has a small effect at lower concentrations and shorter hybridization times, with the 10 min hybridized, 40 mM Mg^{2+} solution having, on average, fewer nanoparticles attaching to the DNA origami than samples with higher Mg^{2+} concentrations. DNA origami solutions with less than 40 mM Mg^{2+} were also studied, but the DNA origami did not adhere to the surface well enough to be evaluated. Some aggregation of Au NPs was observed in the form of clusters of Au NPs on the surfaces. These clusters appeared larger and more frequently on the samples with higher Mg^{2+} concentrations and longer hybridization times (see Figure S1 in the ESI). The best conditions from this study appear to be 70-100 mM Mg^{2+} concentrations and 30-90 min hybridization times.

We note that the 10 and 30 min hybridization time samples in this study on average had more Au NPs attached and smaller gap sizes than those in the more extensive time study in Figure 4 and Table S1. The reason for this is not entirely known, although it probably involves gradual changes in the solution chemistry over time, which was also studied and will be discussed later. The Au NP solution for the Mg^{2+}/hybridization time study was 5 days old, whereas the Au NP solutions for the hybridization time study and varying concentration ratios study were used immediately following filtration.

We also studied changing the ratio of Au NPs to DNA origami; the DNA origami concentration was held constant at a final concentration of 0.2 nM and the concentration of the Au NPs was varied with final concentrations of 4, 8, 20, and 40 nM. For 22 Au NPs attaching to each DNA origami structure, these concentrations correspond to ratios of 0.9:1, 1.8:1, 4.5:1, and 9.1:1 Au NPs per attachment location on the DNA origami structures. Figure 7, and Table S3 in the ESI, show the data for

Au NP placement numbers and gap size. All four samples had a hybridization time of 60 min, within the range of the best working conditions from previous experiments. The effect of changing the concentration of Au NPs was not as pronounced as for changing other conditions, but there appears to be a gradual increase in the number of Au NPs attaching to the DNA origami, along with a decrease in gap sizes with higher Au NP to attachment site ratios.

One notable trend was the increase in numbers of Au NPs not on the DNA origami on the surface as Au NP concentration went up (Fig. S2 in the ESI). This increase in Au NP background is undesirable for subsequent metal plating, as the background Au NPs will also enlarge during the metallization process. However, we note that increasing the concentration of Au NPs could help increase the yield of Au NP attachment without affecting the background if the DNA origami structures were more strongly affixed to the surface, because more rigorous rinsing techniques could be used to remove the excess, unbound Au NPs.

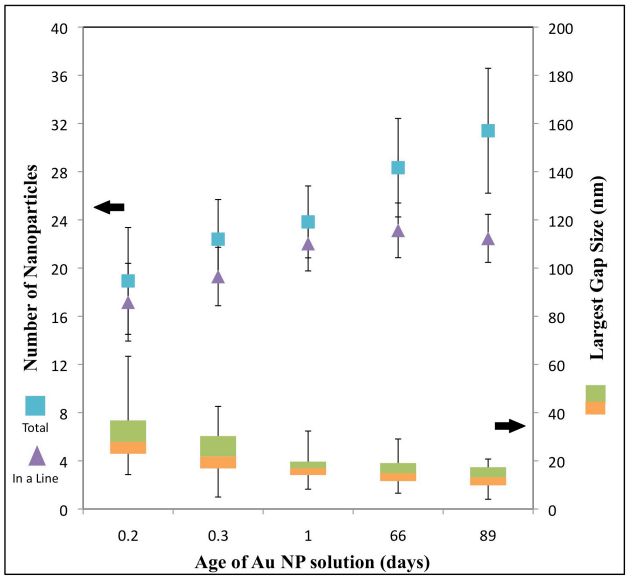

Figure 8. Au NP attachment results with Au NP solutions of different ages. Purple triangles represent the average number of Au NPs along a line. Blue squares represent the average total number of Au NPs per nanostring. Orange and green rectangles are a box and whisker plot of the largest gap between neighboring Au NPs in each nanostring. Thirty nanostrings were counted for each solution age.

Another factor that affects the number of Au NPs attaching to the DNA origami structures is the age of the DNA-coated Au NP solution; specifically, the time since excess unbound thiolated DNA strands have been removed through filtration. In our previously published study,[30] the DNA-coated Au NP solutions were prepared and stored at 4 °C until needed for experiments. Each time the solution was exhausted, more was prepared. However, Kuzyk et al.[29] recently described the importance of filtering the Au NP solution immediately before use to remove DNA strands with oxidized thiols that have desorbed from the Au NPs over time. This prevents these free DNA strands from pairing with the attachment sequences on the DNA origami structures, thereby hindering the Au NPs from attaching. Au NPs could also slowly aggregate in solution after filtration, which would have the opposite effect, allowing multiple Au NPs to deposit by each hybridization site (and more than just in a single line). To test this factor with our structures, we compared samples made with the same hybridization times and solution concentrations, but different ages of the filtered Au NP solution.

The Au NP age data from samples prepared with a 1.8:1 ratio of Au NPs to DNA origami attachment locations, 100 mM Mg^{2+} in the DNA origami solution, and 60 min hybridization times are shown in Figure 8, and Table S4 in the ESI. The total number of Au NPs attached to the DNA origami structures was closer to the number of Au NPs attaching single-file in structures seeded with freshly filtered (≤1 day) Au NP solutions than for older solutions. Aggregation of Au NPs in solution over time could be causing this effect. The DNA origami structures seeded with Au NPs less than 1 day after filtration of the Au NP solution have fewer Au NPs attaching in a single-file arrangement than those more than 1 day old. Adjustment of sample preparation conditions, such as using a longer hybridization time, could address this issue for freshly filtered Au NP samples. There is also a trend toward decreasing largest gap sizes with increasing age of the Au NP solution, which differs from what would be expected if desorbed DNA strands block attachment sites on the DNA origami structures. However, smaller gaps are expected for structures with more Au NPs attached, so Au NP aggregation in older solutions could be filling in some gap regions that might have been expected from blocked attachment sites. Moreover, the lack of Au NP deposition on the base of the "T" structures (i.e., Figs. 2, 3, 5 and 9) shows that hybridization of thiol-linked oligonucleotides to the DNA origami is essential for Au NP placement, including when some aggregation occurs. These results further support the idea that such aggregation and site-specific localization can happen after partial desorption of thiolated oligonucleotides over time.

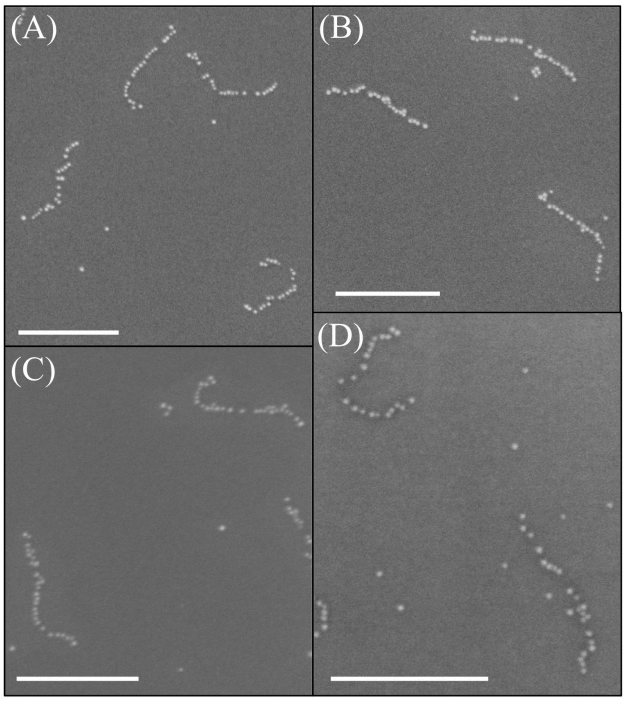

Figure 9. SEM images of Au NP attachment under the range of optimum conditions. The conditions for each sample are as follows: 0.2 nM "T" DNA origami, with (A) 8 nM Au NPs and 100 mM Mg^{2+} in the DNA solution, with a 30 min hybridization time; (B) 8 nM Au NPs and 70 mM Mg^{2+} in the DNA solution, with a 90 min hybridization time; (C) 8 nM Au NPs and 100 mM Mg^{2+} in the DNA solution, with a 90 min hybridization time; (D) 20 nM Au NPs and 100 mM Mg^{2+} in the DNA solution, with a 60 min hybridization time. Scale bars are 200 nm.

As noted earlier, the time between filtering the Au NPs and seeding the DNA origami structures could also explain some of the variations in the data between different sets of experiments. Indeed, the Au NP solution for the Mg^{2+}/hybridization time study was 5 days old and had on average more Au NPs attaching and smaller gap sizes than in either the hybridization-time or varying-concentration-ratio study, in which the Au NP solution was used immediately following filtration.

Figure 9 shows SEM images of Au NP strings, formed under a range of conditions near the optimum. Hybridization times ranging from 30–90 min, Mg^{2+} concentrations of 70–100 mM, and ratios from 1.8–4.5 Au NPs per DNA origami attachment location produce the least aggregated nanostructures with the smallest gaps. There are some small gaps (20 nm median) in these structures and variability within samples, indicating that further improvement is still possible. One reason for the existence of some gaps within the structures seeded under optimized conditions could be that all the attachment sequences are the same. If two different Au NP attachment sequences were used and alternated (i.e., in groups of three) along the seeded section,[29] then the Au NPs would be better directed to specific sites on the DNA structure (Fig. 10). This would eliminate gaps arising from Au NPs attaching and leaving spaces too small for another Au NP to bind (i.e., Figure 1D). Finally, some gaps within the structures in Figure 9 appear large enough (>10 nm) for another Au NP to fit into. These sites may have free DNA strands that paired with the DNA origami and blocked Au NPs from binding in those locations.

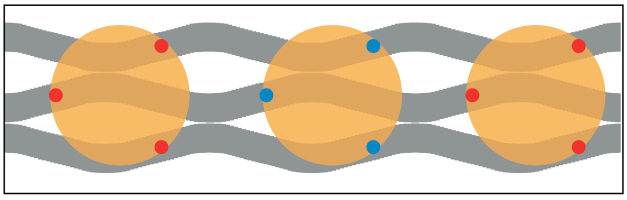

Figure 10. Attachment sequence pattern with two different staple strand extension sequences. Blue and red circles indicate locations where the attachment sequences extend from the staple strands. If at least two different sequences (i.e., red vs. blue) were used and alternated in groups of three, the Au NPs could be directed to specific attachment locations along the "T" DNA origami structures.

Conclusions

In summary, we have studied several experimental parameters to determine the best conditions for densely attaching Au NPs to a targeted portion of a DNA origami structure in a single-file line. Conditions, including the hybridization time, concentration of Mg^{2+} in the DNA solutions, the ratio of Au NPs to DNA origami, and the time since filtration of the Au NP solution, were varied to determine their effects on Au NP attachment. Parameters that were measured via SEM imaging included the number of Au NPs attaching per DNA origami structure, the number of Au NPs attaching single-file, and the largest gap between adjacent Au NPs in the DNA origami.

Reducing the number of unnecessary Au NPs attaching to the DNA origami structures, while also decreasing the distance between the Au NPs, will both contribute to the ability to create thinner and more continuous metallized nanowires after electroless plating. The best conditions we found were between 70–100 mM Mg^{2+} in the DNA origami solutions, ratios from 1.8–4.5 Au NPs per attachment location on the DNA origami structures, and hybridization times ranging from 30–90 min. Assembling DNA templated Au NP structures which allow for even thinner plated nanowires should be possible through the use of alternating different attachment sequences to place the Au NPs more precisely, the use of smaller Au NPs, and/or through improved surface attachment coupled with more rigorous rinsing techniques. Coupled with site-specific semiconductor attachment allowed by DNA origami, these nanowires would be an important step towards the bottom-up construction of nanocircuits.

Acknowledgements

This work was supported by the Semiconductor Research Corporation under contract no. 2013-RJ-2487. We gratefully acknowledge Michael Standing for technical support with electron microscopy. We also express gratitude to Drs. Yanli Geng and Anthony Pearson for their valuable insights and advice.

Notes and references

[a] Department of Chemistry and Biochemistry, Brigham Young University, Provo, Utah 84602, USA.
[b] Department of Chemical Engineering, Brigham Young University, Provo, Utah 84602, USA.

Electronic Supplementary Information (ESI) available: Includes experimental materials and methods as well as supplementary figures and tables. See DOI: 10.1039/b000000x/

1 P. W. K. Rothemund, *Nature*, 2006, **440**, 297.
2 L. Qian, Y. Wang, Z. Zhang, J. Zhao, D. Pan, Y. Zhang, Q. Liu, C. H. Fan, J. Hu and L. He, *Chinese Sci Bull*, 2006, **51**, 2973.
3 E. S. Andersen, M. Dong, M. M. Nielsen, K. Jahn, A. Lind-Thomsen, W. Mamdouh, K. V. Gothelf, F. Besenbacher and J. Kjems, *ACS Nano*, 2008, **2**, 1213.
4 E. Pound, J. R. Ashton, H. A. Becerril and A. T. Woolley, *Nano Lett*, 2009, **9**, 4302.
5 E. S. Andersen, M. Dong, M. M. Nielsen, K. Jahn, R. Subramani, W. Mamdouh, M. M. Golas, B. Sander, H. Stark, C. L. P. Oliveira, J. S. Pedersen, V. Birkedal, F. Besenbacher, K. V. Gothelf and J. Kjems, *Nature*, 2009, **459**, 73.
6 H. Dietz, S. M. Douglas and W. M. Shih, *Science*, 2009, **325**, 725.
7 S. M. Douglas, H. Dietz, T. Liedl, B. Hogberg, F. Graf and W. M. Shih, *Nature*, 2009, **459**, 414.
8 D. Han, S. Pal, J. Nangreave, Z. Deng, Y. Liu and H. Yan, *Science*, 2011, **332**, 342.
9 Y. G. Ke, S. Lindsay, Y. Chang, Y. Liu and H. Yan, *Science*, 2008, **319**, 180.

10 A. Kuzuya, M. Kimura, K. Numajiri, N. Koshi, T. Ohnishi, F. Okada and M. Komiyama, *Chembiochem*, 2009, **10**, 1811.
11 B. Sacca, R. Meyer, M. Erkelenz, K. Kiko, A. Arndt, H. Schroeder, K. S. Rabe and C. M. Niemeyer, *Angew Chem Int Edit*, 2010, **49**, 9378.
12 N. V. Voigt, T. Torring, A. Rotaru, M. F. Jacobsen, J. B. Ravnsbaek, R. Subramani, W. Mamdouh, J. Kjems, A. Mokhir, F. Besenbacher and K. V. Gothelf, *Nat Nanotechnol*, 2010, **5**, 200.
13 Y. G. Ke, J. Nangreave, H. Yan, S. Lindsay and Y. Liu, *Chem Commun*, 2008, 5622.
14 R. Chhabra, J. Sharma, Y. G. Ke, Y. Liu, S. Rinker, S. Lindsay and H. Yan, *J Am Chem Soc*, 2007, **129**, 10304.
15 S. Rinker, Y. G. Ke, Y. Liu, R. Chhabra and H. Yan, *Nat Nanotechnol*, 2008, **3**, 418.
16 A. Kuzyk, K. T. Laitinen and P. Torma, *Nanotechnology*, 2009, **20**, 235305.
17 B. Sacca and C. M. Niemeyer, *Chem Soc Rev*, 2011, **40**, 5910.
18 H. K. K. Subramanian, B. Chakraborty, R. Sha and N. C. Seeman, *Nano Lett*, 2011, **11**, 910.
19 H. A. Becerril and A. T. Woolley, *Chem Soc Rev*, 2009, **38**, 329.
20 E. P. Gates, A. M. Dearden and A. T. Woolley, *Crit Rev Anal Chem*, 2014, **44**, 354.
21 G. P. Acuna, M. Bucher, I. H. Stein, C. Steinhauer, A. Kuzyk, P. Holzmeister, R. Schreiber, A. Moroz, F. D. Stefani, T. Liedl, F. C. Simmel and P. Tinnefeld, *ACS Nano*, 2012, **6**, 3189.
22 G. P. Acuna, F. M. Möller, P. Holzmeister, S. Beater, B. Lalkens and P. Tinnefeld, *Science*, 2012, **338**, 506.
23 J. Sharma, R. Chhabra, C. S. Andersen, K. V. Gothelf, H. Yan and Y. Liu, *J Am Chem Soc*, 2008, **130**, 7820.
24 B. Q. Ding, Z. T. Deng, H. Yan, S. Cabrini, R. N. Zuckermann and J. Bokor, *J Am Chem Soc*, 2010, **132**, 3248.
25 A. M. Hung, C. M. Micheel, L. D. Bozano, L. W. Osterbur, G. M. Wallraff and J. N. Cha, *Nat Nanotechnol*, 2010, **5**, 121.
26 M. Endo, Y. Y. Yang, T. Emura, K. Hidaka and H. Sugiyama, *Chem Commun*, 2011, **47**, 10743.
27 M. Pilo-Pais, S. Goldberg, E. Samano, T. H. LaBean and G. Finkelstein, *Nano Lett*, 2011, **11**, 3489.
28 Z. Zhao, E. L. Jacovetty, Y. Liu and H. Yan, *Angew Chem Int Edit*, 2011, **50**, 2041.
29 A. Kuzyk, R. Schreiber, Z. Y. Fan, G. Pardatscher, E. M. Roller, A. Hogele, F. C. Simmel, A. O. Govorov and T. Liedl, *Nature*, 2012, **483**, 311.
30 A. C. Pearson, J. Liu, E. Pound, B. Uprety, A. T. Woolley, R. C. Davis and J. N. Harb, *J Phys Chem B*, 2012, **116**, 10551.
31 X. B. Shen, C. Song, J. Y. Wang, D. W. Shi, Z. A. Wang, N. Liu and B. Q. Ding, *J Am Chem Soc*, 2012, **134**, 146.
32 W. P. Klein, C. N. Schmidt, B. Rapp, S. Takabayashi, W. B. Knowlton, J. Lee, B. Yurke, W. L. Hughes, E. Graugnard and W. Kuang, *Nano Lett*, 2013, **13**, 3850.
33 S. Pal, Z. T. Deng, B. Q. Ding, H. Yan and Y. Liu, *Angew Chem Int Edit*, 2010, **49**, 2700.
34 H. Bui, C. Onodera, C. Kidwell, Y. Tan, E. Graugnard, W. Kuang, J. Lee, W. B. Knowlton, B. Yurke and W. L. Hughes, *Nano Lett*, 2010, **10**, 3367.
35 S. H. Ko, G. M. Gallatin and J. A. Liddle, *Adv Funct Mater*, 2012, **22**, 1015.